NATIONAL ADVISORY COMMITTEE FOR AERONAUTICS

WARTIME REPORT

ORIGINALLY ISSUED
December 1944 as
Advance Restricted Report L4K22

AERODYNAMIC TESTS OF A FULL-SCALE TBF-1 AILERON INSTALLATION IN THE LANGLEY 16-FOOT HIGH-SPEED TUNNEL

By John V. Becker and Peter F. Korycinski

Langley Memorial Aeronautical Laboratory
Langley Field, Va.

NACA

WASHINGTON

NACA ARR No. L4K22 [redacted]

NATIONAL ADVISORY COMMITTEE FOR AERONAUTICS

ADVANCE RESTRICTED REPORT

AERODYNAMIC TESTS OF A FULL-SCALE TBF-1 AILERON INSTALLATION IN THE LANGLEY 16-FOOT HIGH-SPEED TUNNEL

By John V. Becker and Peter F. Korycinski

SUMMARY

The failure of wing panels on a number of TBF-1 and TBM-1 airplanes in flight has prompted several investigations of the possible causes of failure. This report describes tests in the Langley 16-foot high-speed tunnel to determine whether these failures could be attributed to changes in the aerodynamic characteristics of the ailerons at high speeds. The tests were made of a 12-foot-span section including the tip and aileron of the right wing of a TBF-1 airplane. Hinge moments, control-link stresses due to aerodynamic buffeting, and fabric-deflection photographs were obtained at true airspeeds ranging from 110 to 365 miles per hour.

The aileron hinge-moment coefficients were found to vary only slightly with airspeed in spite of the large fabric deflections that developed as the speed was increased. An analysis of these results indicated that the resultant hinge moment of the ailerons as installed in the airplane would tend to restore the ailerons to their neutral position for all the high-speed flight conditions covered in the tests. Serious aerodynamic buffeting occurred at up aileron angles of -10° or greater because of stalling of the sharp projecting lip of the Frise aileron. The peak stresses set up in the aileron control linkages in the buffeting condition were as high as three times the mean stress.

During the hinge-moment investigation, flutter of the test installation occurred at airspeeds of about 150 miles per hour. This flutter condition was investigated in some detail and slow-motion pictures were made of the motion of the wing tip and aileron. The flutter

[redacted]

was found to involve simultaneous normal bending and chordwise oscillation of the wing and flapping of the aileron. The aileron motion appeared to be coupled with the motion of the wing through the mass unbalance of the aileron in the normal-to-chord plane due to location of the hinge line 2.17 inches below the center of gravity of the aileron. Flutter did not occur when the installation was stiffened to prevent chordwise motion or when the bending frequency of the aileron system was appreciably higher than that of the wing as in the complete airplane installation.

INTRODUCTION

A number of failures of the outer wing panel of the TBF-1 and TBM-1 airplanes have occurred in pull-outs from shallow dives. These failures occurred at the wheel wells and could not be explained simply on the basis of excessive pull-out loading. The theory was advanced that the high-speed aerodynamic characteristics of the aileron system might be such as to cause the aileron control to become unstable at the speeds attained in the pull-outs, with the result that the ailerons would suddenly assume full deflection and thereby overload the wing.

The principal purpose of the present tests was to investigate the aileron hinge-moment characteristics at high speeds in order to determine whether the aileron system could have been responsible for the wing failures in flight. The Langley 16-foot high-speed tunnel was chosen for the investigation because airspeeds in excess of the airplane pull-out speeds could be obtained and because the tunnel is large enough to accommodate a section of the airplane wing including the aileron.

Inspection of a number of TBF-1 airplanes had indicated minor differences in the aileron installations due to manufacturing variations. In order to evaluate the possible effect of such variations on the hinge-moment characteristics, two complete series of tests were made - one with the aileron hinge line adjusted so that the aileron would be in its correct position with respect to the wing contour and the other with the hinge line and aileron lowered 1/4 inch.

At high negative aileron angles, serious aerodynamic buffeting was encountered in the tests. Strain gages installed on one of the aileron control links provided data on the stress increments due to the buffeting.

In the early stages of the investigation, flutter of the test installation occurred. This flutter condition and means for eliminating it were studied in some detail with the aid of the strain-gage installation used in the buffeting measurements and also by means of slow-motion pictures.

Motion pictures were also made of the deflection of the fabric on the upper surface of the aileron for all the hinge-moment tests in order to permit correlation between any changes in hinge-moment coefficient and aileron shape.

SYMBOLS

H_a	aileron hinge moment, foot-pounds
C_{h_a}	aileron hinge-moment coefficient $\left(\frac{H_a}{qb_a\overline{c_a}^2}\right)$
δ_a	aileron angle, degrees
S_w	wing area, square feet
$\overline{c_a}$	root-mean-square chord of aileron behind hinge line, feet
b_a	aileron span, feet
c_w	wing chord, feet
q	dynamic pressure, pounds per square foot $\left(\frac{1}{2}\rho V^2\right)$
V	true airspeed, miles per hour or feet per second
V_i	arbitrarily called indicated airspeed, miles per hour or feet per second $\left(\frac{1}{2}\sigma V\right)$
α	angle of attack of wing, degrees
f	frequency, cycles per minute

f_a aileron bending frequency, cycles per minute

f_f flutter frequency, cycles per minute

C_L lift coefficient (Lift/qS_w)

M Mach number (V/a)

a speed of sound in air, miles per hour or feet per second

σ density ratio (ρ/ρ_o)

ρ mass density of air, slugs per cubic foot

ρ_o mass density of air at sea level (0.002378 slug/cu ft)

APPARATUS AND METHODS

Test model.- A 12-foot-span section including the tip and aileron of the right outer wing panel of a TBF-1 airplane was used in the tests. The principal dimensions of the model are

Wing section	NACA 230 series
Model wing span, feet	11.84
Maximum chord, feet	8.71
Tip chord, feet	4.58
Area of model wing, square feet	78.70
Aileron span, feet	7.63
Location of aileron hinge line	$0.80c_w$
Aileron chord behind hinge line	$0.20c_w$
Root-mean-square aileron chord behind hinge line, $\overline{c_a}$, feet	1.27

Wing mounting.- The wing was mounted from the left wall of the test section of the tunnel as shown in figures 1 and 2. In the vicinity of the attachment fitting, the wing was reinforced by $\frac{3}{32}$-inch dural plates extending about 2 feet spanwise and from the 10-percent-chord to the 50-percent-chord stations. These plates were riveted to the stringers and to the spar flanges. The end of the wing section was covered by a steel plate $\frac{1}{8}$ inch thick

attached by means of $\frac{3}{4} \times \frac{3}{4} \times \frac{1}{16}$-inch angles to the skin and stringers. The reinforced section of the wing covering and the main spar were bolted into a steel plate $\frac{5}{8}$ inch thick by means of $2 \times 2 \times \frac{1}{4}$-inch steel angles. (See fig. 3.) This plate was rigidly clamped to the tunnel structure. It should be noted that, in the chordwise direction, the support fitting terminated at the main spar and at the 10-percent-chord station. Beyond these points, the wing did not contact the tunnel structure, except in a few runs in which a block was inserted at about the 80-percent-chord station between the wing and the tunnel wall in order to produce extreme chordwise rigidity. (See fig. 2.) Without this block in place the wing, rotating as a solid body about the support fitting, could be made to oscillate in the chordwise direction.

Aileron.- The aileron was of the Frise type. (See fig. 4.) With the wing at zero angle of attack and the aileron neutral, the center of gravity of the aileron was located 2.17 inches vertically above the hinge line, 0.24 inch forward of the hinge line, and 41 inches from the inboard end of the aileron. The weight of the aileron was 28.7 pounds. The spacing of the ribs was unequal with the outermost section of the aileron having the maximum distance between ribs. (See fig. 1.)

Hinge-moment measurement.- The hinge-moment forces of the aileron were transmitted to a suitable balance through the linkage in the section of the wing tested. The fourth link inboard from the aileron extended out of the wing. The force in this link was transmitted through a bell crank to the balance. A direct calibration of the system was made by applying known hinge moments to the aileron. In determining the aileron angle for a particular test condition, allowance was made for deflections in the aileron linkage system. The aileron angles shown in this report are believed to be correct within about $\pm 0.2^{\circ}$ for the steady test conditions.

Strain gage.- A temperature-compensated strain gage was installed on the second link of the aileron control system inboard from the aileron. This link was essentially a 12-inch turnbuckle with a barrel $7\frac{5}{8}$ inches long and 1 inch in diameter. The link was pin-jointed at its ends so that the loads indicated by the strain gage corresponded

to principal tension or compression loads. Strain-gage records were obtained for all the runs, including those in which flutter occurred, and were used to obtain the relative stresses in the link and the flutter frequency. These strain-gage traces were also used to verify that the vibration was continuous and of the flutter type and not merely a random or irregular vibration due to buffeting.

Lift determination.- As previously stated the wing was attached to the tunnel wall and, therefore, forces on the wing could not be measured with the wind-tunnel balance system. It was necessary, however, to obtain approximate values of the lift in order to prevent overloading of the model and also to permit the evaluation of tunnel-wall effects. The lift was obtained from measurements of the deflection of the wing tip. A calibration of this deflection against the total lift load was obtained from a static-load test in which the wing was loaded with sand bags.

Natural bending frequencies.- The natural bending frequency of the wing structure as installed in the tunnel was considerably greater than that of the wing panel mounted on the airplane. Vibration-frequency data were obtained by shaking the wing with a variable-speed motor coupled to the wing with a rubber band about 1/8 inch in diameter. The natural bending frequencies thus determined were as follows:

(1) Principal bending mode normal to the chord line with small component in chordwise direction

$$f = 755 \text{ cycles per minute}$$

(2) Principal bending mode in chordwise plane with small component normal to chord

$$f = 960 \text{ cycles per minute}$$

(3) Torsion mode

$$f = 2840 \text{ cycles per minute}$$

Modes (1) and (3), respectively, involved bending and twisting of the wing structure. Mode (2), however, consisted of oscillation of the wing as a solid body about its support mounting.

The critical bending frequency of a complete wing installed on a TBF-1 airplane was measured as 500 cycles per minute. In order to make the frequency of the principal bending mode the same for the tunnel installation as for the airplane, 76.4 pounds of lead were bolted to the wing structure as shown in figure 2. The critical bending frequencies then measured were as follows:

(1) Principal bending mode normal to the chord line with small component in chordwise direction

f = 500 cycles per minute

(2) Principal bending mode in chordwise plane with small component normal to chord

f = 600 cycles per minute

During the flutter tests, the aileron control tube (the fourth control link inboard from the aileron) was attached to the tunnel structure through cantilever springs of various stiffnesses as shown in figure 5. The natural vibration frequency of the aileron control system could be varied by this means from 400 to 800 cycles per minute. The value measured on a TBF-1 airplane with control stick fixed was 680 cycles per minute. The various steel cantilever springs were 2 inches wide by $8\frac{1}{2}$ inches long. The aileron frequencies for various spring thicknesses, measured in the same manner as the wing frequencies except as noted, are as follows:

Spring thickness (in.)	Aileron frequency (cpm)
0.25	420, [a]400
.30	500, [a]470
.35	535, [a]575
.25 and 0.35 clamped together	620
.30 and 0.35 clamped together	680
∞ (link clamped to wall)	800

[a]Obtained by deflecting aileron spring and measuring resulting oscillations when spring was released.

TESTS

Hinge moment.- The hinge-moment data were obtained with the wing set at angles of attack of -1.2°, 3.5°, and 8.0°. For each angle of attack, a range of aileron angles from approximately -20° to 18° was covered. High negative angles could be obtained only at low test speeds because of the severe buffeting encountered. The maximum allowable positive angles were determined by lift limit imposed by structural considerations. At the highest test speed (365 mph), for example, an aileron angle of only 11° could be obtained for $\alpha = -1.2°$. The strain-gage and motion-picture data were obtained simultaneously with the hinge-moment data. These test conditions were covered both with the normal hinge line and with the hinge line and aileron lowered 1/4 inch.

Flutter.- Flutter tests were made with and without the 76.4-pound weight in the wing tip. A range of aileron bending frequencies was covered for each of these two conditions. Various aileron angles were tested for each combination of wing and aileron bending frequency. A few additional runs were made with the installation greatly stiffened in the chordwise plane by the insertion of a steel block between the wing and the tunnel wall at approximately the 80-percent-chord station. The usual test procedure was to set the angle of attack of the wing and the aileron angle and then increase the tunnel speed until flutter appeared or until it became evident that there would be no tendency to flutter. In many of the runs the spring in the aileron control system was deflected and suddenly released, or triggered, in order that any tendency to flutter could be detected before the actual flutter speed was reached.

Test Mach numbers.- The tests were run at constant values of $\sigma^{\frac{1}{2}}V$, which is arbitrarily defined as indicated airspeed. The corresponding approximate test Mach numbers and true airspeeds for the average test conditions are

$\frac{1}{\sigma^2 V}$ (mph)	M	V (mph)
110	0.12	112
160	.21	166
210	.28	217
260	.36	275
310	.44	333
335	.48	365

DISCUSSION

Hinge Moments

Jet-boundary corrections.- The effects of the jet boundary on the hinge-moment coefficients were studied with the aid of reference 1. Of the several factors affecting the hinge moment, only the effect of streamline curvature was found to be of appreciable magnitude. For the model tested, the value of the correction is approximately $0.015C_L$. By using the lift coefficients from figure 6, the values of this correction were computed and added to the uncorrected values of the hinge-moment coefficients. The corrected hinge-moment data presented herein represent the aileron characteristics that would be obtained in free air for a complete wing with the same semispan dimensions as the test model. The aspect ratio of this equivalent wing is 3.5, and the ailerons cover a larger proportion of the span than on the actual airplane. Exact agreement between the present test data and flight data for the actual airplane is therefore not to be expected.

Variation with airspeed.- The data of figures 7 to 9 show surprisingly little effect of increasing airspeed on the hinge-moment coefficients. This result was obtained in spite of large fabric deflections that occurred at the higher airspeeds. Typical fabric deflections are shown in figure 10, which was obtained from enlargements of 16-millimeter motion-picture records. Previous investigations have shown that fabric deflections generally have

an appreciable effect on hinge moments. Important scale and compressibility effects have also been noted. The absence of any net effect for the present installation may be explained by the possibility that the action of the several contributing factors was compensatory in this particular case. In any event, it is clear that no high-speed control difficulties due to radical changes in aileron characteristics will occur for flight Mach numbers up to 0.48.

Effect of hinge-line location.- Comparison of figures 7 to 9 shows that lowering the aileron and the hinge line 1/4 inch had an appreciable effect on the curves of hinge-moment coefficient, particularly for small aileron deflections. Under high-speed flight conditions in which only small aileron deflections are employed, a marked reduction in stick force would be noted for the ailerons in the lowered position as compared with the normal position. This result emphasizes the need for small installation tolerances for this type of aileron in high-speed airplanes if the desired handling characteristics are to be obtained.

Effect of lift coefficient.- The effects on the hinge-moment coefficient of increasing the wing lift coefficient may be seen by comparing the results of figures 7 to 9 for a given aileron angle. The value of $\partial C_{h_a}/\partial C_L$ at $\alpha = 0^\circ$ and $\delta_a = 0^\circ$ is approximately 0.04 for both normal and lowered positions of the aileron. The lift coefficients corresponding to the angles of attack of figures 7 to 9 are shown in figure 6 as mean curves that were faired through test points for all airspeeds. It should be mentioned that the downwash effect on the slope of the lift curve is larger for the low equivalent aspect ratio of the test model than for the airplane; that is, the angle of attack for a given lift coefficient is considerably greater than in flight. In view of the impossibility of obtaining accurate direct lift measurements with the test installation, it was considered justifiable not to apply jet-boundary corrections to the lift data of figure 6.

Aileron control characteristics.- The net aileron control moment in the airplane is the resultant of the aerodynamic moments due to the upgoing and downgoing ailerons. It is obviously desirable that this resultant

moment should always tend to return the ailerons to their neutral positions. This condition occurs if the quantity $C_{h_{\text{up aileron}}} - C_{h_{\text{down aileron}}}$ has a positive value for all control positions. If the ailerons are assumed to be rigged at $\delta_a = 0^\circ$ and the deflection of the up aileron is assumed to be approximately equal to the deflection of the down aileron, it can be seen from figures 7 to 9 that the ailerons would tend to return to neutral for all the conditions of the tests. Furthermore, the resultant moment increases continuously with aileron deflection. There would thus be no tendency for any type of aileron control snatch in any control position or flight condition. This conclusion is arrived at without consideration of elastic deflection of the aileron control system. The principal effect of elasticity is to produce unequal deflections of the ailerons, the downgoing aileron tending to have smaller deflections because of its larger hinge moments. For the ailerons tested, allowance for this effect does not change the foregoing conclusion that the resultant aerodynamic control moment tends to restore the ailerons to neutral for all control-stick deflections. It appears possible, however, that the resultant restoring moment for a part of the range of control motion might decrease with increasing stick deflection at very high speeds. While this latter condition represents an undesirable high-speed control characteristic, it does not seem likely that it would lead to catastrophic results.

Elastic instability of aileron control system at very high speeds.- The possibility that the aileron control system might become elastically unstable at very high speeds is now investigated. The primary requirement for elastic instability resulting in aileron snatch is that the curve of aileron hinge-moment coefficient, as conventionally plotted against aileron angle, shall have a region of positive slope. The divergent condition occurs when the change in aerodynamic hinge moment per degree change of aileron angle $\partial H_a/\partial \delta_a$ equals the stiffness of the control system with fixed control stick expressed in terms of hinge moment required per degree change of aileron angle. The condition can be visualized by imagining the existence of a hinge moment large enough to produce 1° of aileron deflection by stretching the aileron control linkages; the larger hinge moment existing with the increased aileron deflection then produces an additional 1° deflection, which in turn produces a larger

hinge moment, and so forth. As a basis for calculating the airspeed at which the divergent condition would occur, the stiffness of the aileron control system on a TBF-1 airplane was measured with the control stick fixed. The value of the stiffness was 16.7 foot-pounds per degree aileron deflection. The condition for divergence was therefore

$$\frac{\partial H_a}{\partial \delta_a} = 16.7$$

In terms of hinge-moment coefficient,

$$\frac{\partial C_{h_a}}{\partial \delta_a} \left(q b_a \overline{c_a}^2\right) = \frac{\partial H_a}{\partial \delta_a}$$

$$= 16.7$$

whence,

$$\frac{\partial C_{h_a}}{\partial \delta_a} = \frac{530}{V_i^2}$$

where V_i is in miles per hour.

The value of $\partial C_{h_a}/\partial \delta_a$ required for divergence has been plotted against indicated airspeed in figure 11. Also plotted in figure 11 is the maximum positive value of $\partial C_{h_a}/\partial \delta_a$ determined from the plots of hinge-moment coefficient. This value, which equals 0.0021, was taken from figure 8 for $\delta_a = -8^\circ$. The divergent condition is not reached with the aileron tested until an indicated airspeed of about 500 miles per hour has been attained. This critical speed is well beyond the limits of operation of the TBF-1 airplane.

Aerodynamic Buffeting

The sharp upturn in the curves of hinge-moment coefficient in figures 7 to 9 at aileron angles of -10° to -14°

is due to separation of the air flow from the lower surface of the aileron starting at the sharp lip that projects at aileron angles of -5° or greater. The data shown in figures 7 to 9 indicate only mean values of the hinge-moment coefficients and give no indication of the unsteady flow conditions that actually occurred. As the flow separated, the hinge moment momentarily increased to a high positive value that, owing to elasticity of the control linkages, reduced the negative angle of the aileron. With the smaller angle, the separated condition and the hinge moments were reduced so that the aileron again tended to assume a larger negative angle. This process repeated continuously. The instantaneous stresses in the control links were much higher for this buffeting condition than the mean values corresponding to the data of figures 7 to 9. The peak instantaneous stress increments have been expressed as effective hinge-moment-coefficient increments in figure 12. Less intense buffeting also occurred at high positive aileron angles because of the separation of the flow on the upper surface. The buffeting tendency of Frise ailerons has been mentioned in reference 2.

The data shown in figure 12 were obtained at indicated airspeeds ranging from 110 to 335 miles per hour. The hinge-moment increments due to buffeting were found to increase as the square of the indicated airspeed, so that ΔC_{h_a} due to buffeting was constant with airspeed. Comparison of the buffeting increments with the mean values of the hinge-moment coefficients of figures 7 to 9 shows that the buffeting increments at high negative angles are several times the mean values in magnitude. This result indicates that test data for Frise ailerons which show only mean values of the hinge-moment coefficient may be dangerously misleading if used as design data for stress-analysis purposes. For the present case, the mean value of the hinge moment for high negative angles should be multiplied by approximately 3 to obtain a conservative value of the effective stress for use in design.

The hinge-moment coefficients for the upgoing aileron (negative aileron angles) are low up to the point at which buffeting begins. This condition therefore is obtainable at very high speeds at which high downgoing-aileron deflections could not be obtained because of the elasticity of the control system. This buffeting condition

may have been a contributing factor to the structural failures occurring in flight in pull-outs from high-speed dives.

Flutter

Flutter conditions.- The results shown in tables I(a) and I(b) indicate that flutter usually occurred when the natural bending frequencies of the wing and aileron were approximately equal. The frequency of the flutter was approximately equal to the natural frequency of the wing in the normal-to-chord mode regardless of the ratio of aileron frequency to wing frequency. When the aileron frequency was reduced below that of the wing (run 594-1), the speed at which flutter occurred was increased but the flutter condition was not definitely eliminated. Increasing the aileron frequency to about 1.4 times the principal bending frequency of the wing eliminated the flutter condition, as may be seen from a comparison of runs 599-1 and 600-3 (table I(b)). The frequency combination of run 600-3 was identical with that measured on a TBF-1 airplane and no flutter occurred for this combination.

Figures 13 and 14 show the change in flutter characteristics with variation in aileron angle. The severity of the flutter tended to decrease as the aileron angle was increased positively. At an aileron angle of 20°, the flutter had degenerated into an irregular vibration of small amplitude. It may also be noted that the flutter frequency tended to increase slightly as the aileron angle was increased. The disappearance of the flutter condition at high aileron angles is believed to be due to an effective stiffening of the aileron system as a result of changes in the aerodynamic characteristics of the aileron. At high aileron angles, the negative slope of the curve of hinge-moment coefficient against aileron angle is much greater than at low angles. (See figs. 7 to 9.) This aerodynamic stiffening had the same general effect on the flutter as the stiffening produced by increasing the thickness of the aileron control spring; that is, the flutter condition was eliminated when the effective aileron bending frequency became appreciably greater than the wing frequency.

Table I(c) shows that no flutter occurred when the chordwise motion of the wing was eliminated by stiffening

the wing mounting, regardless of the ratio of aileron frequency to wing frequency.

Analysis of flutter mode.- As previously noted, the aileron was mass-balanced in the conventional manner; that is, the center of gravity of the aileron was forward of the hinge line. Aileron flutter of the usual type in which normal wing bending is coupled with deflections of the aileron was therefore impossible. In order to determine the nature of the flutter occurring in these tests, the aileron and wing tip were photographed during flutter with a motion-picture camera at the rate of 64 frames per second. The motion of the wing tip and aileron was then charted from an analysis of consecutive photographs. Figure 15 illustrates the results of this study for 1 cycle of the flutter motion. It may be seen that the wing tip traveled in an elliptical path. No torsional deflection of the wing was evident. The x- and y-components of several cycles of the motion shown in figure 15 are plotted against time in figure 16, and the corresponding motion of the aileron is also shown. It may be noted that the magnitude of the chordwise component was approximately equal to the magnitude of the normal component and that the two components were only slightly out of phase. The aileron motion was approximately 90° out of phase with the bending components; that is, deviation of the aileron from its mean position (-7°) was approximately zero at either extreme of the bending motion of the wing, and the maximum deviation of the aileron occurred when the wing was near its neutral position. The direction, or sign, of the aileron deviation was such as to maintain the flutter, as may be seen from either figure 15 or figure 16. If it is assumed that there is no lag in the aerodynamic forces, the 90° phase relationship between wing and aileron motion would probably produce the maximum amount of excitation for the flutter motion.

As previously mentioned, the results shown in table I indicate that the chordwise motion of the wing was essential to the flutter. Two possible mechanisms by which the chordwise motion might be coupled with the aileron motion so as to produce the flutter condition are

(1) With the control linkage terminating in a structure that is fixed relative to the wing, chordwise motion of the wing produces relative motion between the wing and control link and hence motion of the aileron

(2) The mass unbalance of the aileron in the normal-to-chord plane would produce deflections of the aileron when chordwise accelerations occurred

In order to investigate the first possibility, the aileron angles that would result from the chordwise displacement component of figure 15 were computed from calibration data obtained under static conditions. The aileron angles so computed are shown in figure 16. The magnitude of the computed aileron motion is only about 7 percent of the magnitude of the actual motion and the phase relationships are not such as to promote the flutter motion. It is therefore concluded that the flutter condition was not related to any peculiarity of the aileron control linkage arrangement used in the tunnel tests.

The second possibility - coupling of the aileron motion and the chordwise motion through the mass unbalance of the aileron in the normal-to-chord plane - is now considered. By referring to the curve of chordwise component in figure 16, it can be determined that a rearward acceleration of the wing existed for all positive values of the chordwise component and a forward acceleration for all negative values. Figure 16 also shows that the aileron motion was in the negative, or upward, direction for the entire period of time during which the rearward acceleration occurred and in the positive direction when the forward acceleration occurred. With the center of gravity of the aileron 2.17 inches above the hinge line, it is clear that a rearward acceleration would be expected to produce motion of the aileron in the negative direction and vice versa, exactly as has been shown to occur in figure 16. The chordwise motion of the wing was therefore directly coupled to the aileron motion, which in turn was of the correct phasing to sustain the flutter condition, as has been previously pointed out. It thus appears that the flutter could have been eliminated in the tests by mass-balancing the aileron in the normal-to-chord plane as well as by the other methods.

Validity of tunnel test results for the actual airplane.- The results of these wind-tunnel flutter tests are not quantitatively applicable to the TBF-1 airplane under flight conditions, principally because only a small section of the complete wing panel was tested. Attention should be directed, however, to the fact that the type of mounting for the test panel was similar to the method of

attachment of the complete outer wing panel on the airplane. In both cases there is no attachment fitting behind the 40-percent-chord station (center line of main spar web). The principal requirements for the flutter condition - lack of chordwise rigidity and mass unbalance of the aileron in the normal-to-chord plane - are thus present in both the airplane and in the tunnel setup. Differences exist, however, in the rigidity of the structures to which the panels were attached and in the moments of inertia of the panels about their mounting points. The ratio of the natural bending frequency in the chordwise plane to that in the normal-to-chord plane might be quite different for the airplane and for the test model. In any event, it is clear that vibration tests of the airplane should be made in order to determine the characteristics of the natural bending modes for comparison with those of the wind-tunnel model. If it is found that the airplane is subject to the same type of flutter as the model, the method of eliminating the flutter in the wind tunnel should be applied to the airplane.

CONCLUSIONS

The results of the investigation of a 12-foot-span section including the tip and aileron of the right wing of a TBF-1 airplane in the Langley 16-foot high-speed tunnel indicated the following conclusions:

1. The hinge-moment coefficients varied only slightly with airspeed in spite of the large fabric deflections that occurred at high speeds for the large aileron angles.

2. Aerodynamic buffeting due to separation of the air flow from the lower surface of the aileron occurred at up aileron angles of -10° or greater. The peak stresses set up in the aileron control linkages because of buffeting were as high as three times the mean stress indicated by conventional hinge-moment balance measurements. This buffeting condition appeared to be the only aerodynamic characteristic that could possibly result in structural failures at high speeds.

3. The hinge-moment coefficients were appreciably affected by lowering the aileron and hinge line 1/4 inch below their normal positions.

4. An analysis of the hinge-moment data showed that the resultant control moment of similar ailerons installed in the airplane would tend to restore the ailerons to their neutral position for all the test conditions.

5. Calculations showed that elastic instability of the aileron control system resulting in snatch of the upgoing aileron would not occur at indicated airspeeds below 500 miles per hour for an aileron with the characteristics measured in the present tests.

6. Wing-aileron flutter involving wing deflection components (both normal and parallel to the chord line) occurred in these tests when the principal natural vibration frequencies of the wing (both normal-to-chord component and chordwise component) were of approximately the same magnitude as the natural bending frequency of the aileron system.

7. The flutter condition was eliminated in the tests either by stiffening the aileron system until its natural bending frequency was at least 1.4 times the principal normal-to-chord wing bending frequency (the frequency ratio measured on a TBF-1 airplane was approximately 1.4) or by greatly stiffening the wing mounting in the chordwise plane.

8. An analysis of the flutter motion as determined from photographs taken at intervals of 1/64 second indicated that the flutter condition could also have been eliminated by mass-balancing the aileron in the normal-to-chord plane. The center of gravity of the aileron as tested was 2.17 inches above the hinge line.

Langley Memorial Aeronautical Laboratory
National Advisory Committee for Aeronautics
Langley Field, Va.

REFERENCES

1. Swanson, Robert S., and Toll, Thomas A.: Jet-Boundary Corrections for Reflection-Plane Models in Rectangular Wind Tunnels. NACA ARR No. 3E22, 1943.

2. Rogallo, F. M.: Collection of Balanced-Aileron Test Data. NACA ACR No. 4A11, 1944.

TABLE I.- FLUTTER TEST RESULTS

Run	α (deg)	f_a (cpm)	δ_a (deg)	$\frac{1}{2}\sigma V$ (mph)	f_f (cpm)	Remarks
(a) Natural vibration frequencies of wing: normal to chord, 755 cpm; chordwise, 960 cpm						
588-1	-1.2	800	0	208	750	Violent flutter
589-1	-1.2	800	0	156	750	Flutter - minimum speed at which flutter could be started at this angle
590-1	-1.2	800	-5	145	735	Flutter
591-1	-1.2	800	5	145	790	Do.
592-1	-1.2	800	10	145	805	Do.
593-1	-1.2	800	20	160	830	Flutter not continuous
593-3	-1.2	800	20	-----	-----	No flutter - maximum test speed, 195 mph
594-1	-1.2	535	0	230	710	Incipient flutter
595-1	3.5	800	0	-----	-----	Some tendency to flutter at 145 and 191 mph; maximum test speed, 235 mph - no flutter
595-2	3.5	800	-5	125	800	Flutter
595-3	3.5	800	-5	145	790	Do.
595-4	3.5	800	-10	148	770	Do.
595-5	3.5	800	-10	156	770	Do.
595-6	3.5	800	5	-----	-----	Some tendency to flutter at 188 mph; maximum test speed, 242 mph - no flutter
596-2	3.5	680	-5	-----	-----	Some tendency to flutter at 147 mph; maximum test speed, 210 mph - no flutter
596-1	3.5	535	-5	-----	-----	No flutter - maximum test speed, 209 mph
(b) Natural vibration frequencies of wing: normal to chord, 500 cpm; chordwise, 600 cpm						
597-1	3.5	500	0	-----	-----	No flutter - maximum test speed, 235 mph
597-2	3.5	500	-5	145	518	Flutter - started by triggering
597-3	3.5	500	5	-----	-----	No flutter
598-1	3.5	535	5	150	525	Flutter
598-2	3.5	535	-5	-----	-----	No flutter - maximum test speed, 210 mph
599-1	-1.2	535	0	164	525	Flutter - started by triggering
599-2	-1.2	535	0	173	525	Do.
599-3	-1.2	500	0	140	525	Do.
599-5	-1.2	500	-5	143	515	Flutter
599-6	-1.2	500	5	120	525	Do.
599-7	-1.2	500	10	100	534	Do.
599-8	-1.2	500	10	128	534	Do.
600-1	-1.2	420	0	140	512	Do.
600-2	-1.2	420	0	159	512	Do.
600-3	-1.2	680	0	-----	-----	No flutter - maximum test speed, 210 mph
(c) Wing restrained from chordwise motion by means of steel block shown in fig. 2						
579-1	-1.2	500	0	160	-----	Wing bending frequency, 500 cpm - no flutter
579-2	-1.2	500	0	210	-----	Do.
579-3	-1.2	500	0	260	-----	Do.
579-4	-1.2	500	0	310	-----	Do.
579-5	-1.2	500	0	335	-----	Do.
580-1	-1.2	500	-5	160	-----	Do.
581-1	-1.2	500	-5	235	-----	Do.
582-1	-1.2	535	-5	185	-----	Do.
582-2	-1.2	535	-5	210	-----	Do.
582-3	-1.2	535	-5	235	-----	Do.
583-1	-1.2	535	0	185	-----	Do.
583-2	-1.2	535	0	200	-----	Do.
583-3	-1.2	535	0	235	-----	Do.
587-1	-1.2	800	-15	160	-----	Wing bending frequency, 755 cpm - no flutter
587-2	-1.2	800	0	210	-----	Do.
587-3	-1.2	800	-5	210	-----	Do.
587-4	-1.2	800	-10	210	-----	Do.

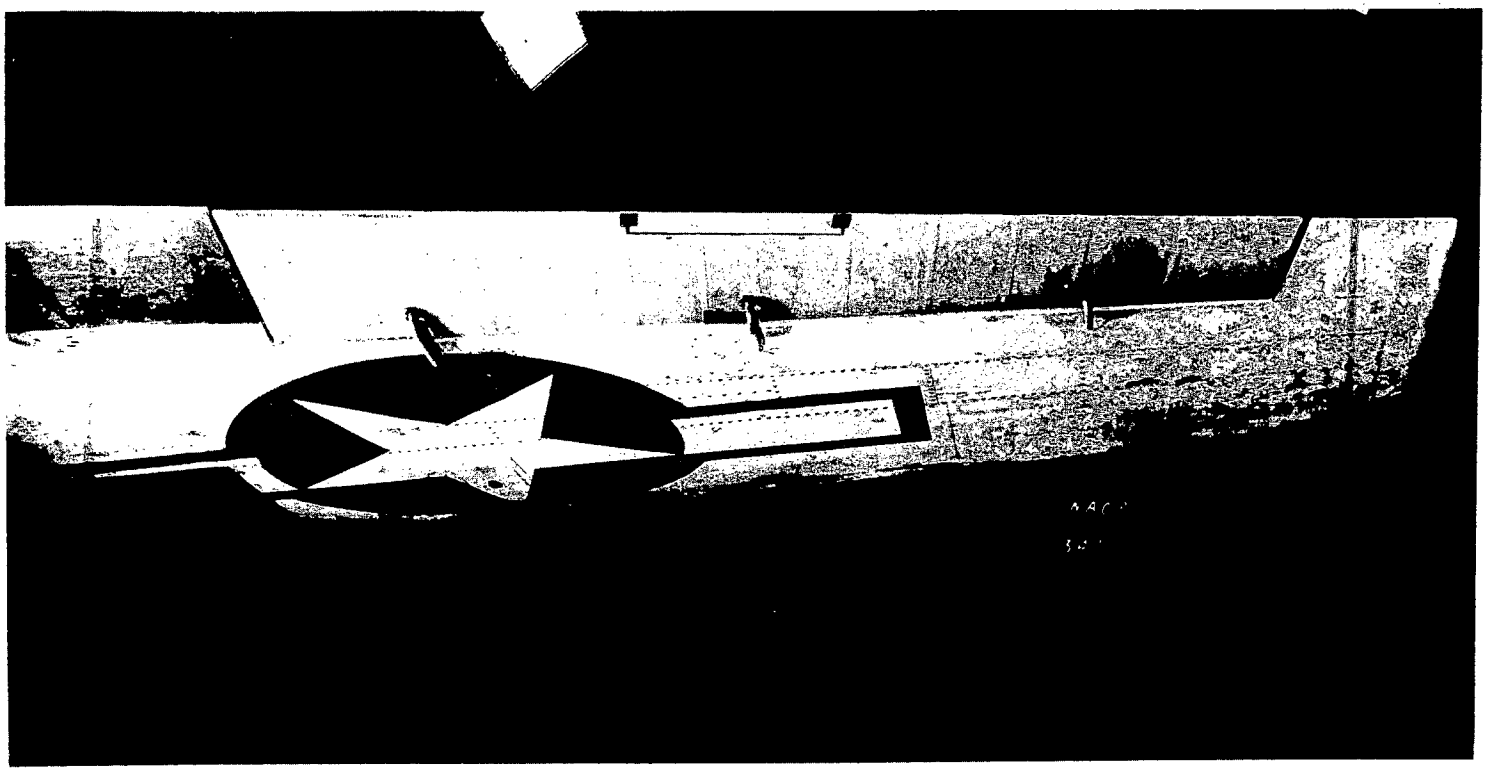

Figure 1.- Installation of a section of the TBF-1 wing in the Langley 16-foot high-speed tunnel.

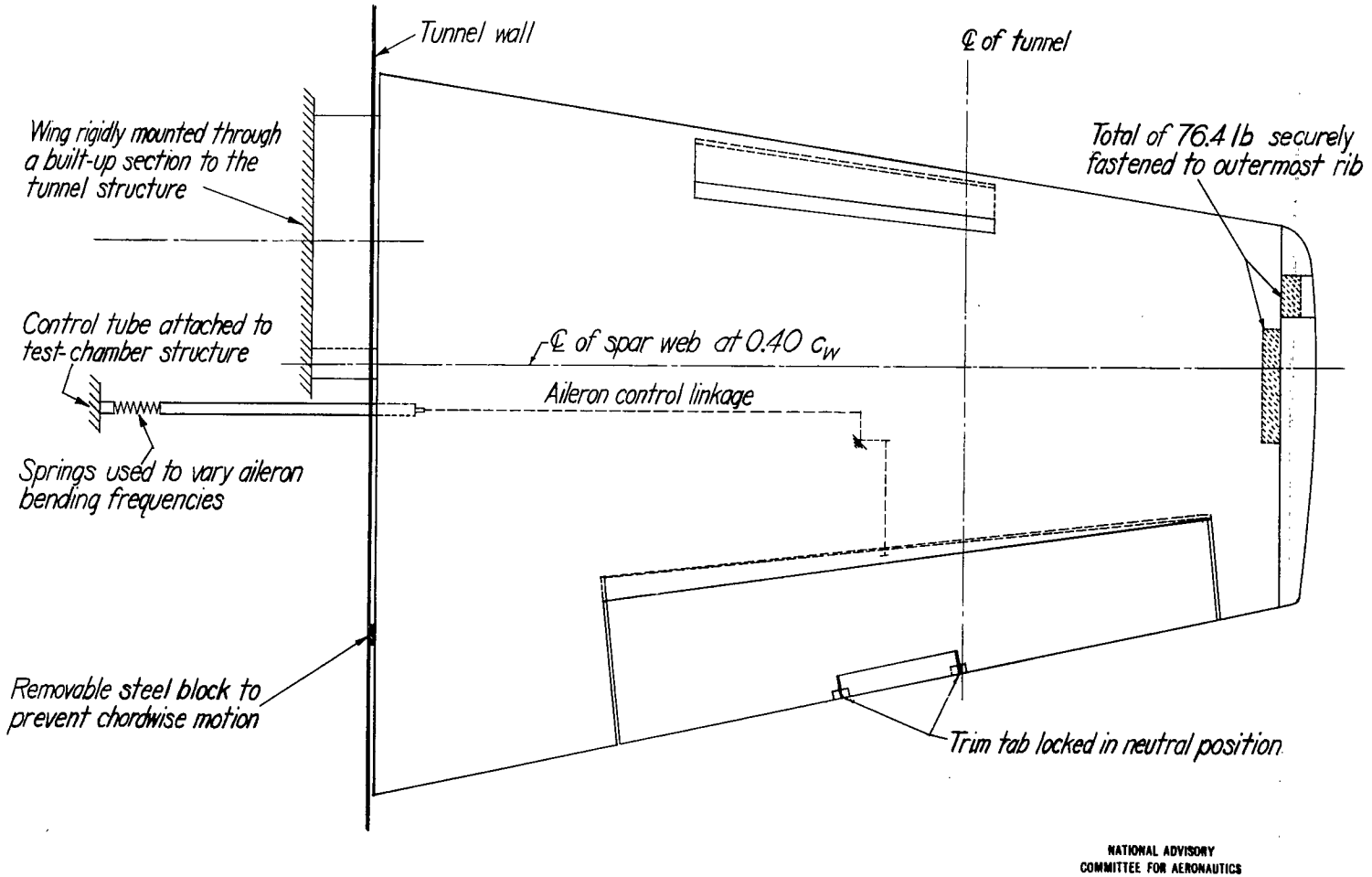

Figure 2.- Installation of section of TBF-1 wing panel for flutter tests in Langley 16-foot high-speed tunnel.

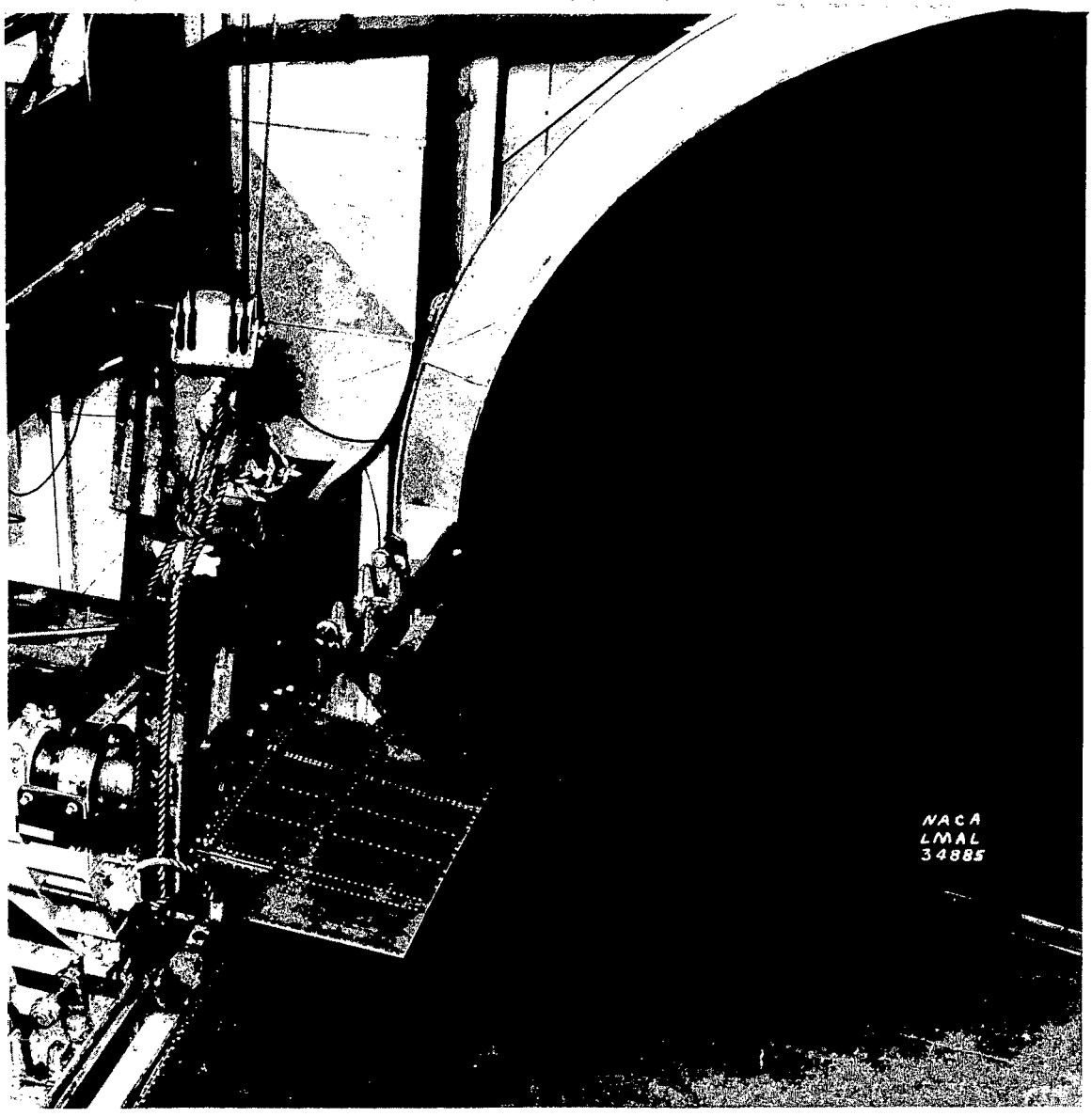

Figure 3.- Method of reinforcement and attachment of wing for tunnel testing.

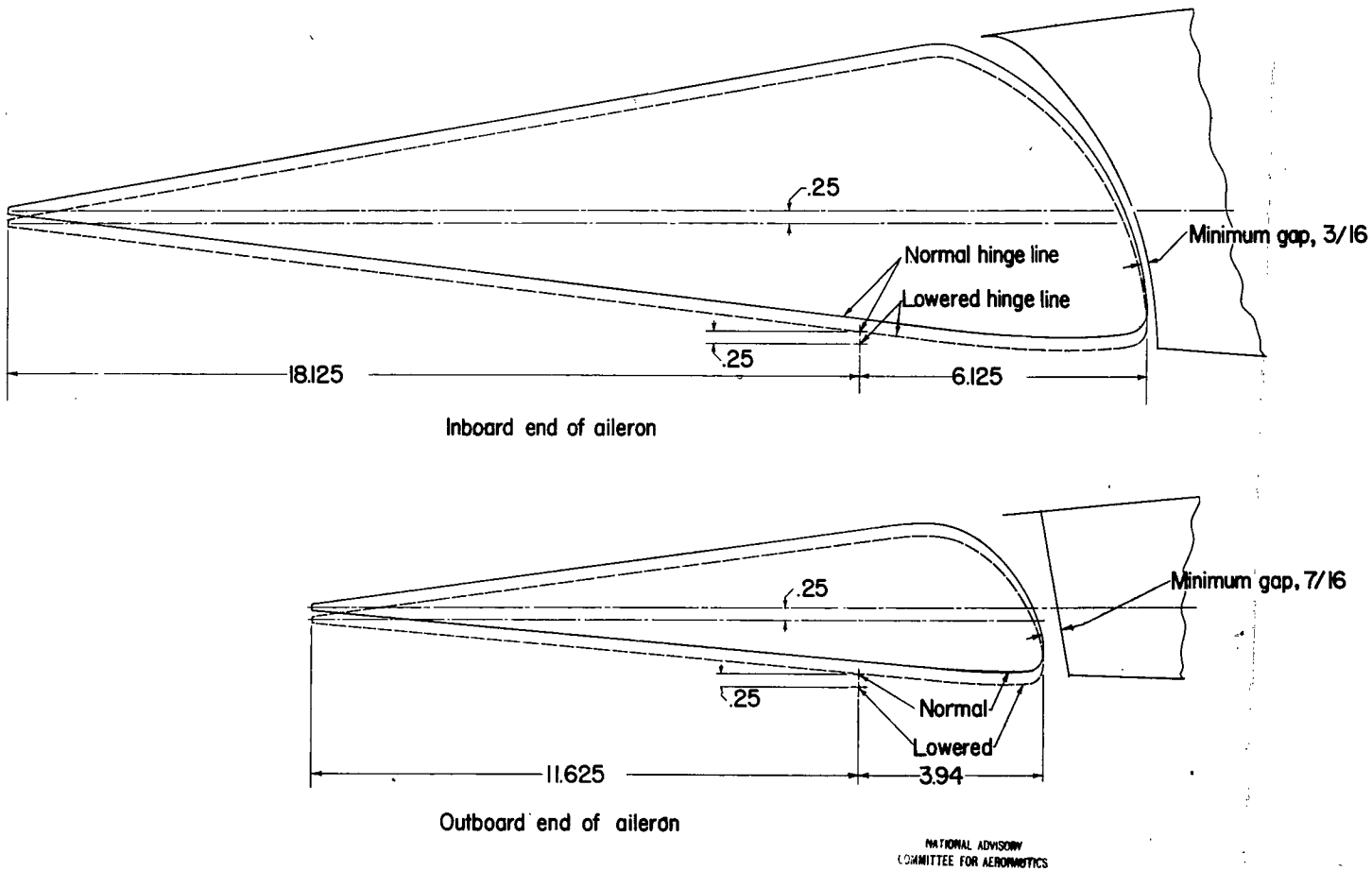

Figure 4.- Aileron end profiles with normal and lowered hinge lines. All dimensions are in inches.

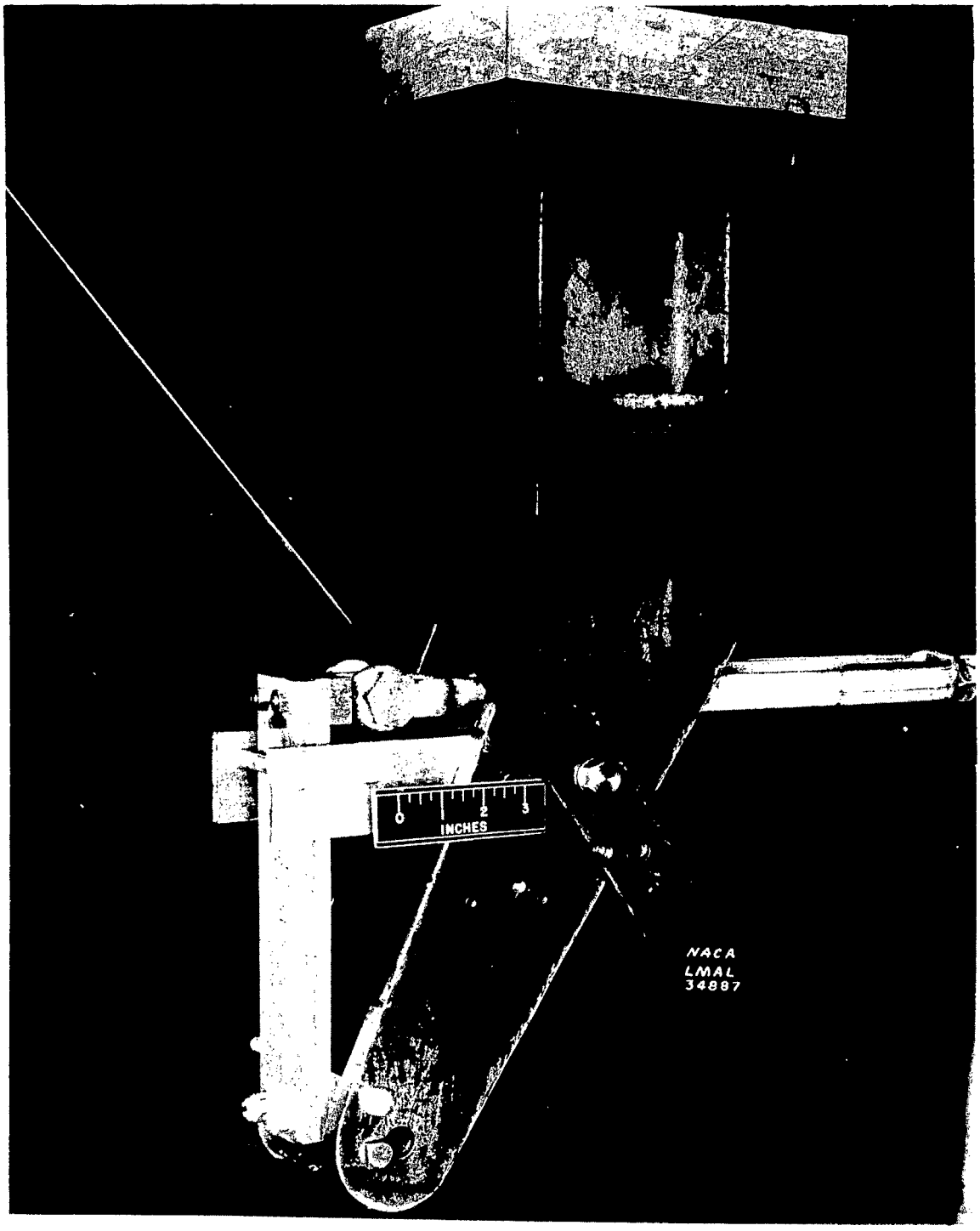

Figure 5.- Cantilever spring used to vary aileron frequency.

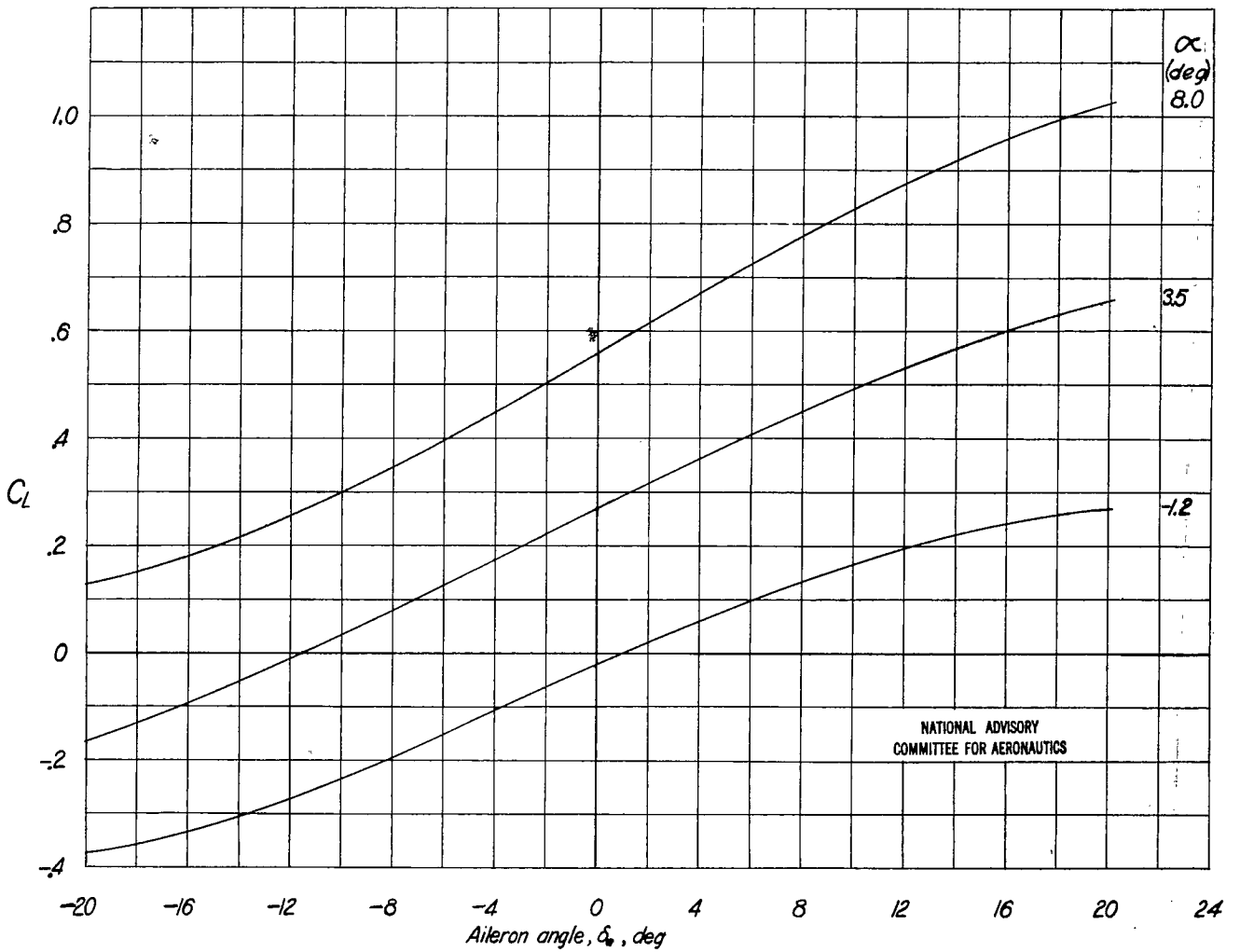

Figure 6.- Variation of lift coefficient with aileron angle for angles of attack of -1.2°, 3.5°, and 8.0°.

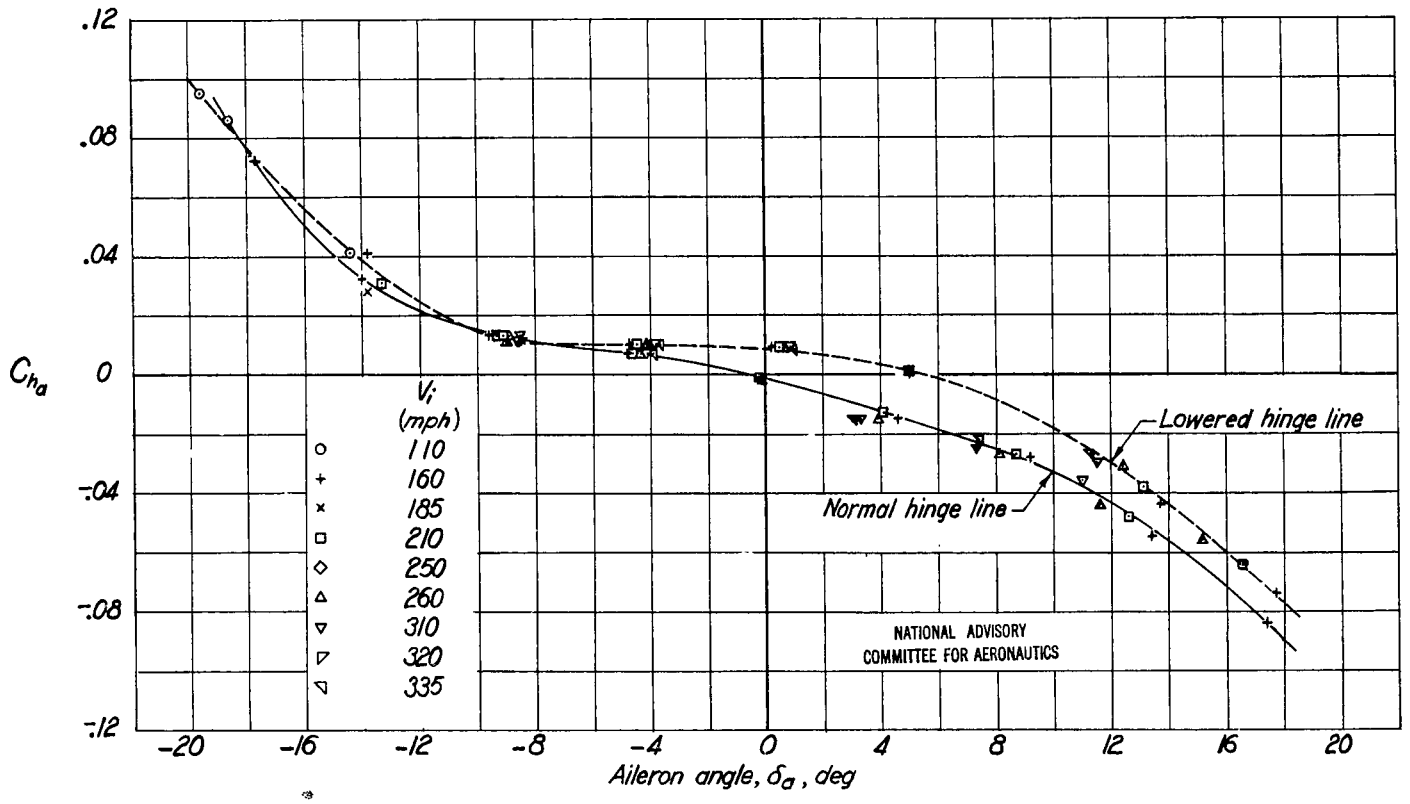

Figure 7.- Variation of aileron hinge-moment coefficient with aileron angle. Normal and lowered hinge lines; angle of attack, -1.2°.

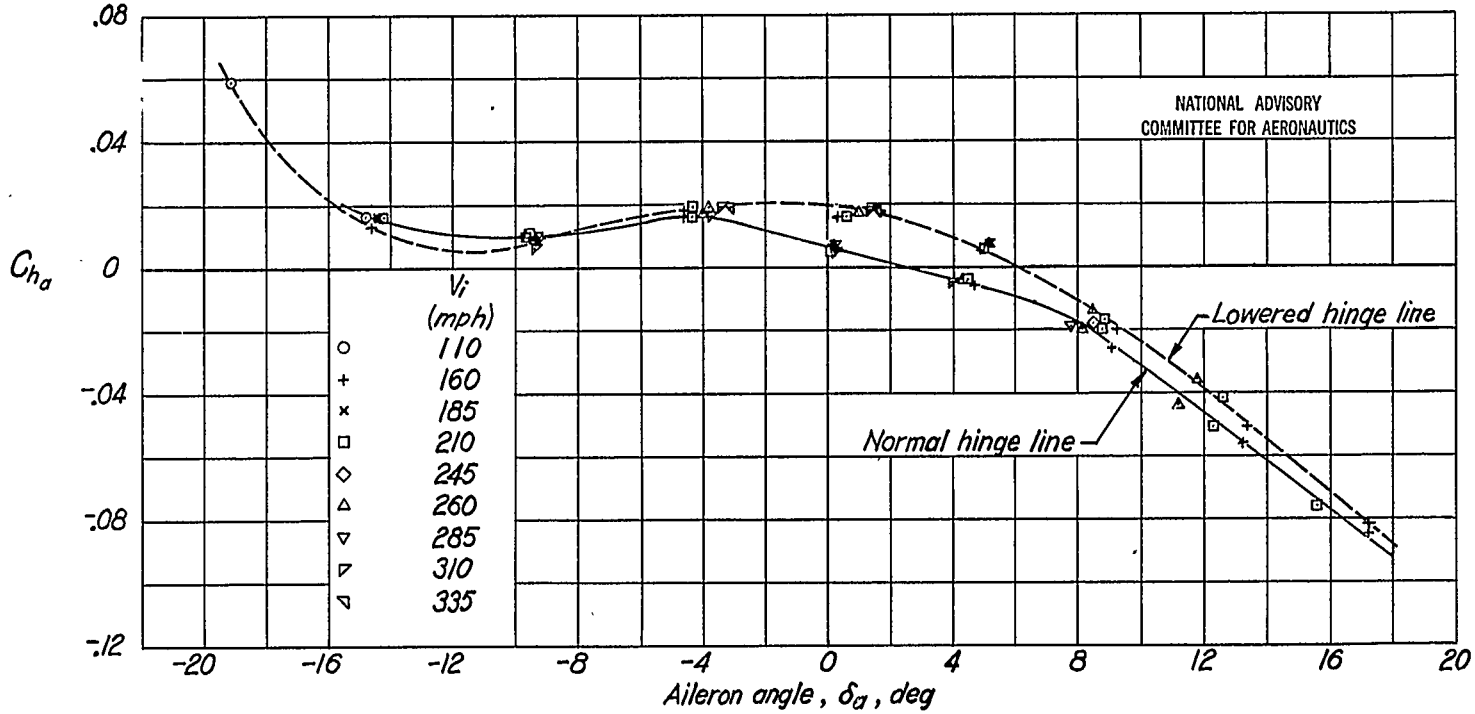

Figure 8.- Variation of aileron hinge-moment coefficient with aileron angle. Normal and lowered hinge lines; angle of attack, 3.5°.

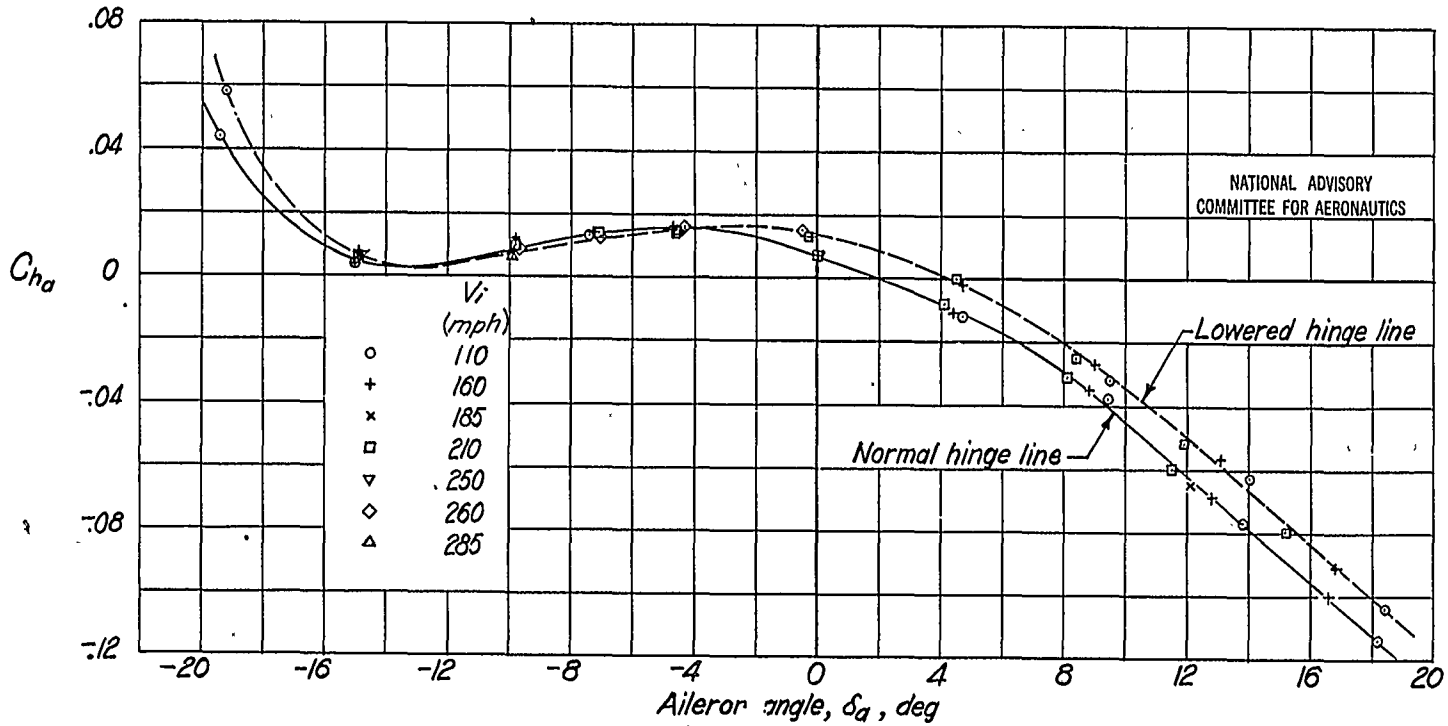

Figure 9.- Variation of aileron hinge-moment coefficient with aileron angle. Normal and lowered hinge lines; angle of attack, 8.0°.

$\alpha = -1.2^{\circ}$; $\delta_a = 0^{\circ}$; $V_i = 160$ mph

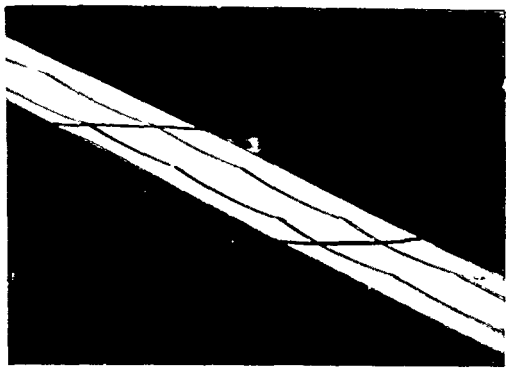

$\alpha = 8^{\circ}$; $\delta_a = -9.9^{\circ}$; $V_i = 285$ mph

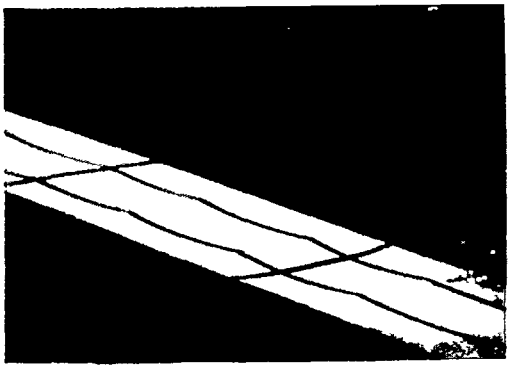

$\alpha = -1.2^{\circ}$; $\delta_a = -8.5^{\circ}$; $V_i = 310$ mph

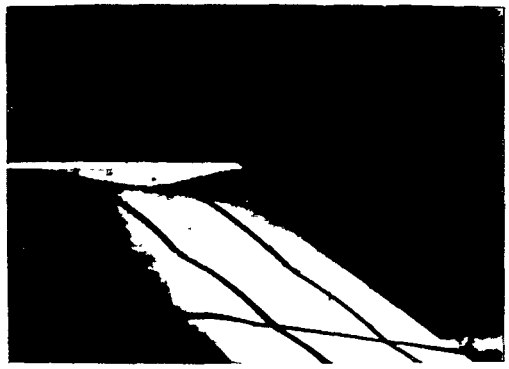

$\alpha = -1.2^{\circ}$; $\delta_a = 8.8^{\circ}$; $V_i = 310$ mph

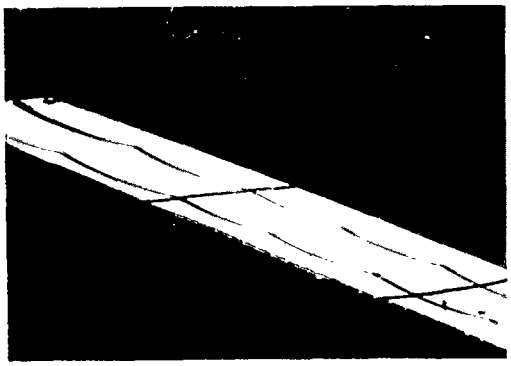

$\alpha = 3.4^{\circ}$; $\delta_a = -9.4^{\circ}$; $V_i = 310$ mph

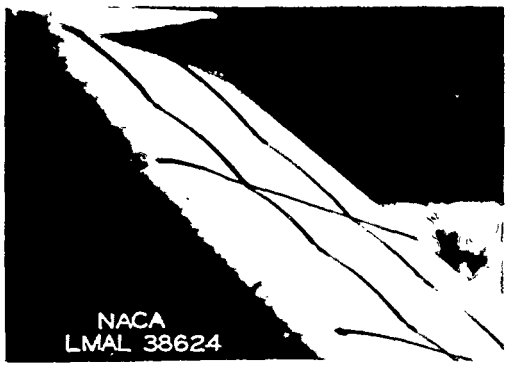

$\alpha = -1.2^{\circ}$; $\delta_a = 15.2^{\circ}$; $V_i = 260$ mph

Figure 10.- Fabric deflections for typical test conditions.

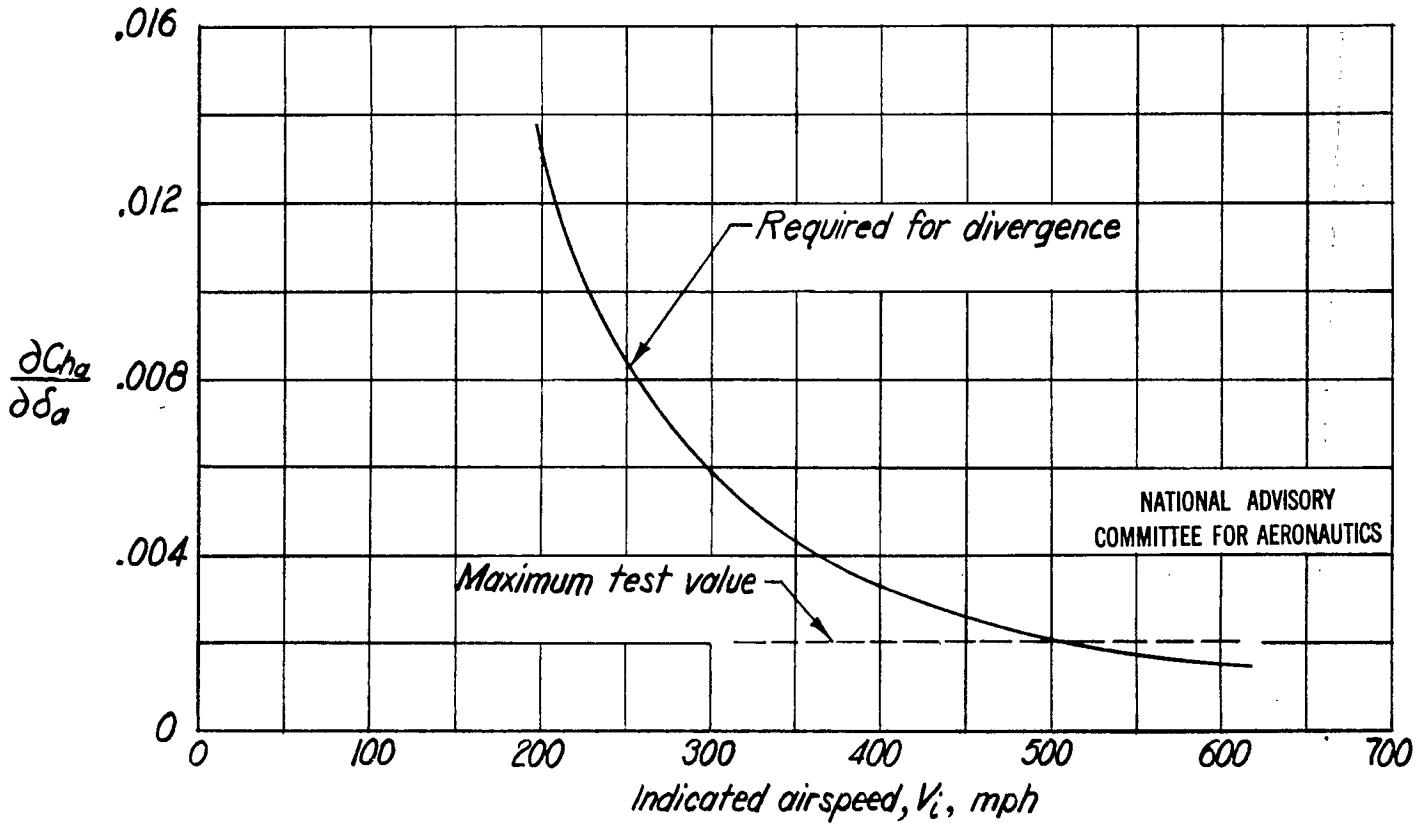

Figure 11 :-Comparison of positive values of slope of hinge-moment-coefficient curve required for divergence in aileron control system with maximum test value.

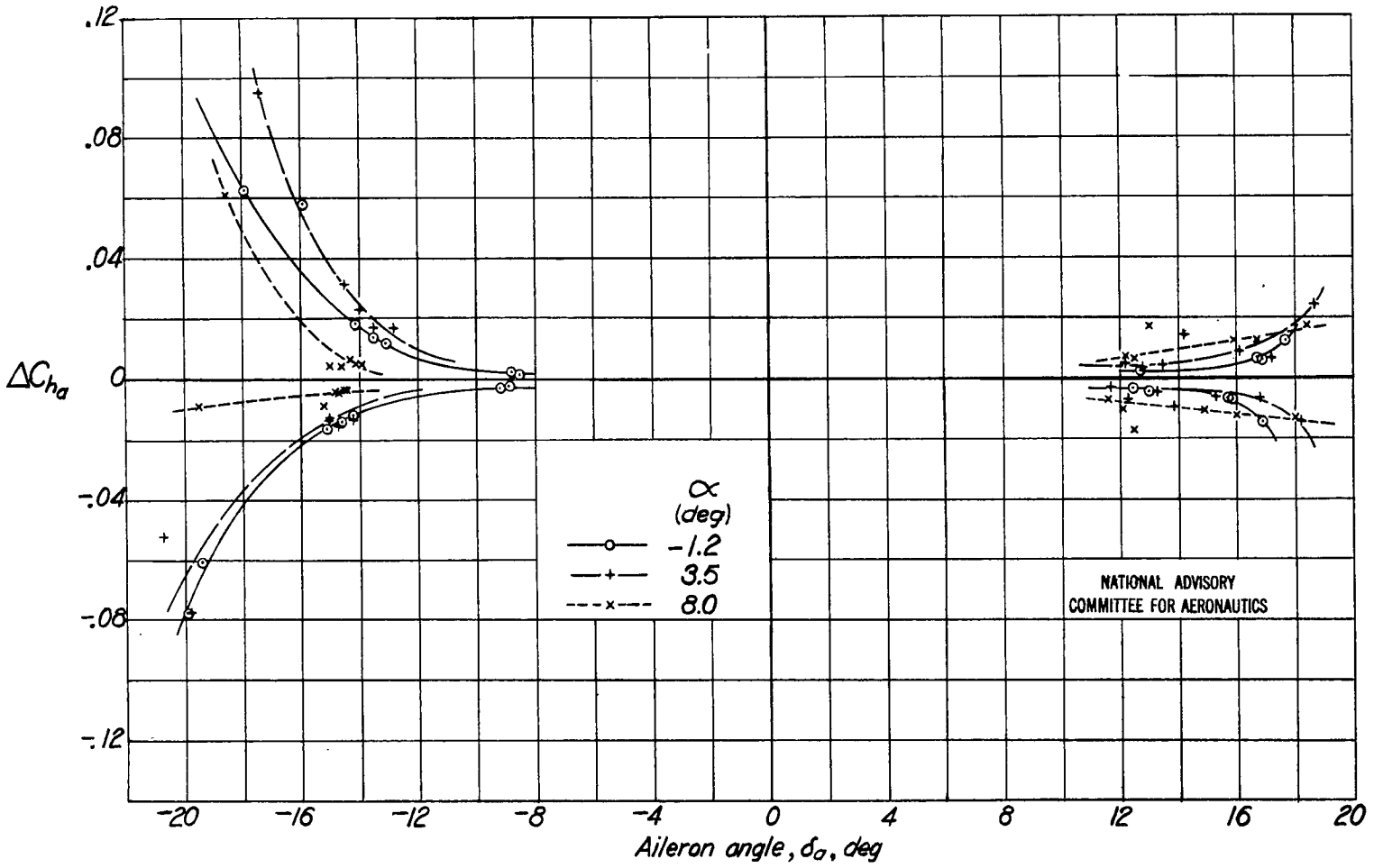

Figure 12.- Increment of aileron hinge-moment coefficient due to aerodynamic buffeting.

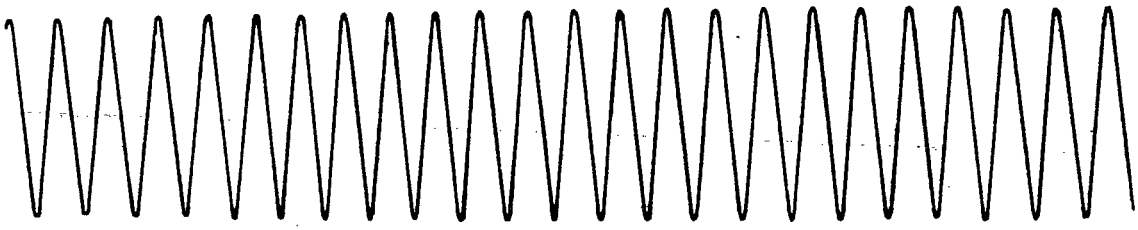

$\delta_a = -5^\circ$; V_i = 145 mph; f_f = 740 cpm

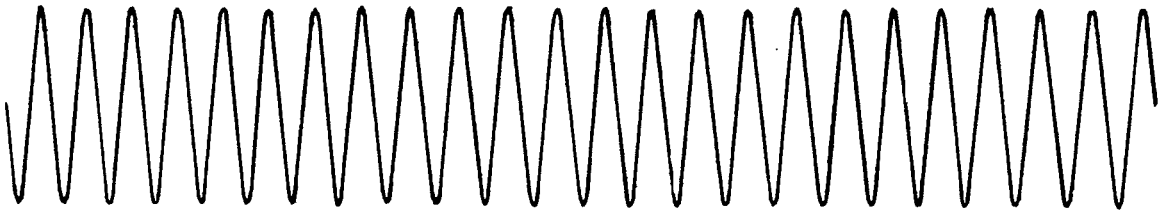

$\delta_a = 0^\circ$; V_i = 156 mph; f_f = 744 cpm

$\delta_a = 5^\circ$; V_i = 145 mph; f_f = 780 cpm

$\delta_a = 10^\circ$; V_i = 145 mph; f_f = 810 cpm

$\delta_a = 20^\circ$; V_i = 160 mph; f_f = 840 cpm

NATIONAL ADVISORY
COMMITTEE FOR AERONAUTICS

Figure 13.- Strain-gage traces. Natural normal-to-chord wing bending frequency, 755 cpm; angle of attack of wing, -1.2°.

$\delta_a = -5^\circ$; $V_i = 143$ mph; $f_f = 515$ cpm

$\delta_a = 0^\circ$; $V_i = 140$ mph; $f_f = 525$ cpm

$\delta_a = 5^\circ$; $V_i = 120$ mph; $f_f = 525$ cpm

NATIONAL ADVISORY
COMMITTEE FOR AERONAUTICS

$\delta_a = 10^\circ$; $V_i = 128$ mph; $f_f = 535$ cpm

Figure 14.- Strain-gage traces. Natural normal-to-chord wing bending frequency, 500 cpm; angle of attack of wing, -1.2°.

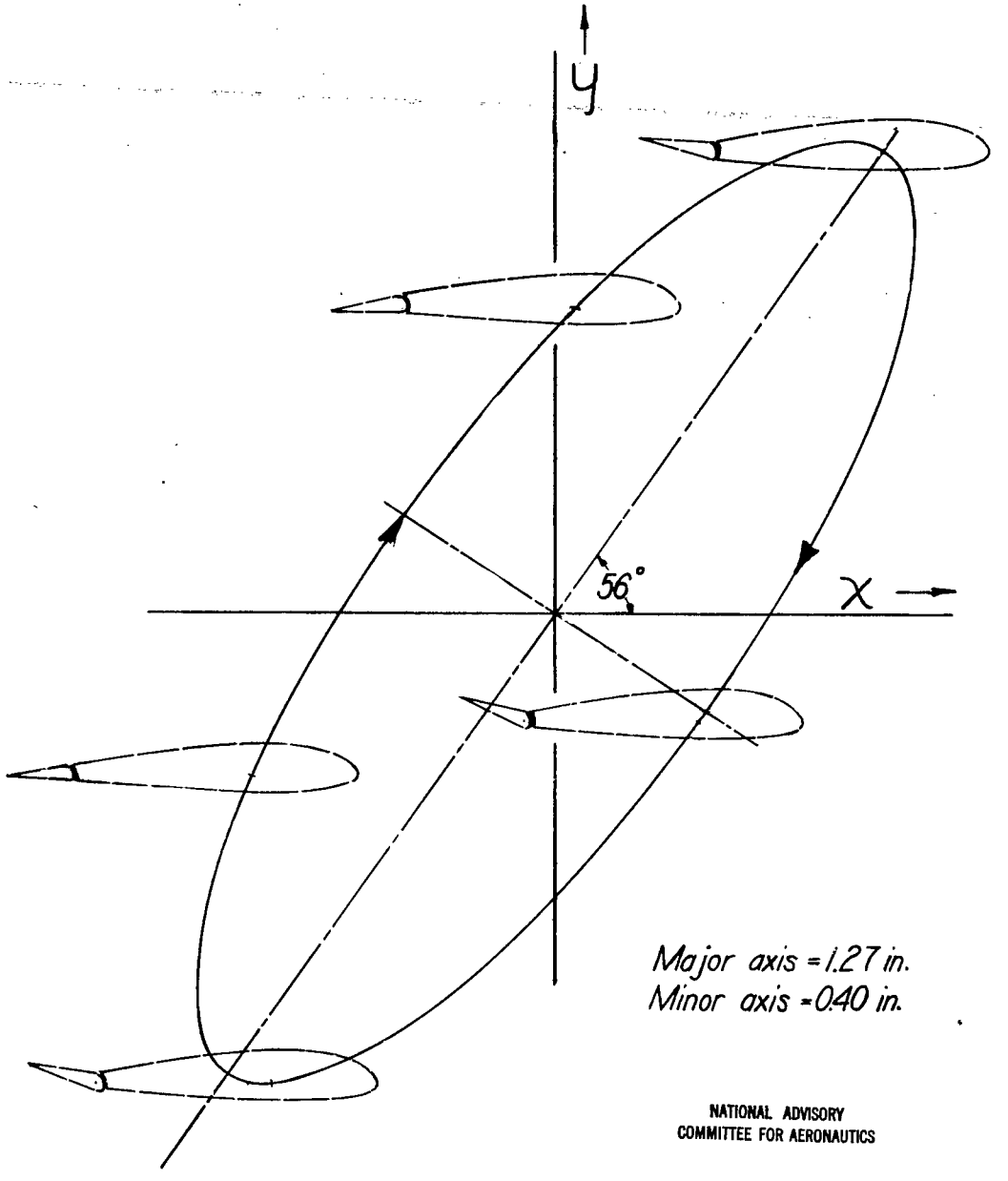

Figure 15.- Enlarged diagram of the motion of wing tip and aileron during flutter. Time interval between positions of wing shown, approximately 1/64 sec; wing angle of attack, 3.5°; mean aileron angle, -7°; indicated airspeed, 155 mph; wing frequency, 755 cpm; aileron frequency, 800 cpm; flutter frequency, 770 cpm.

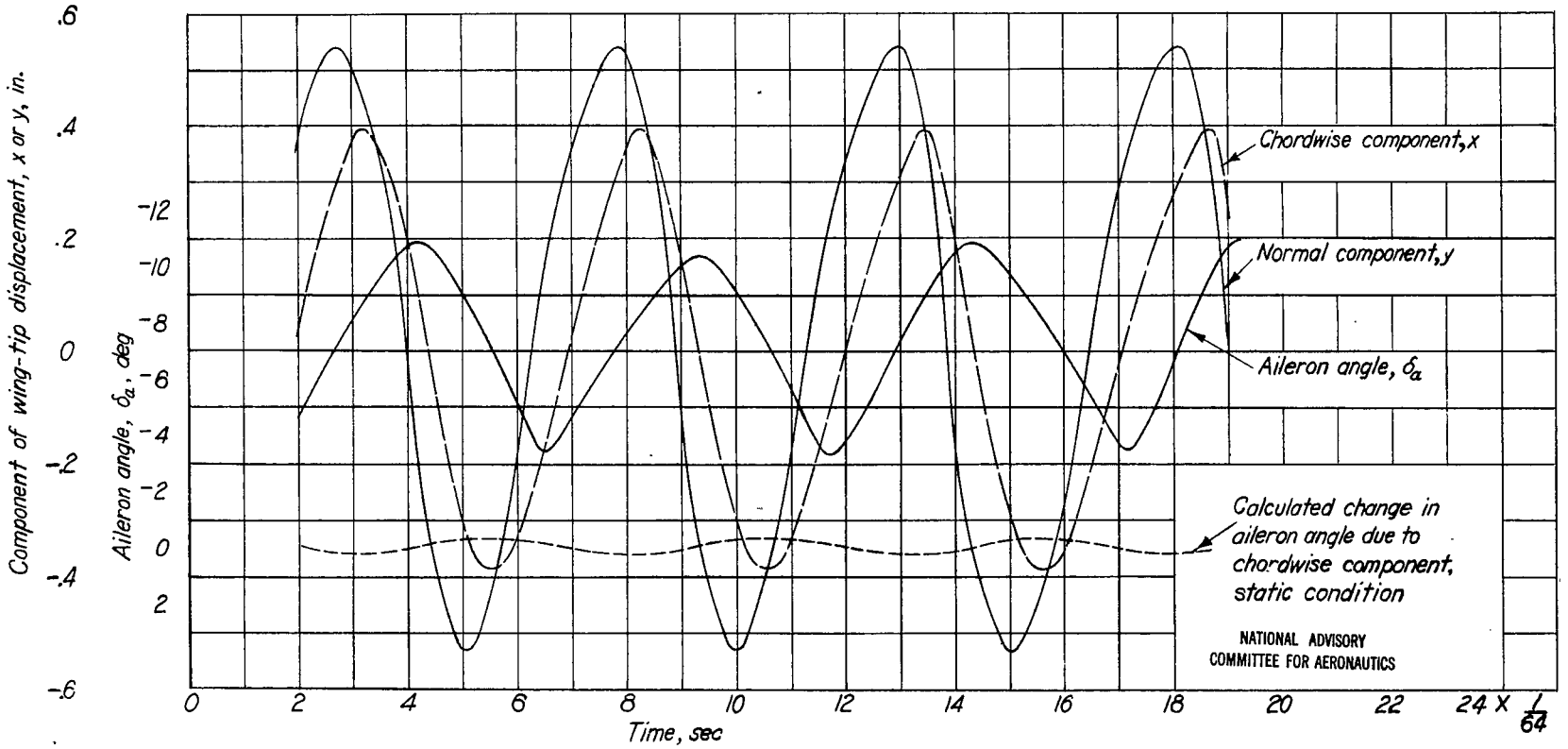

Figure 16.-Normal and chordwise components of flutter motion and aileron angle as functions of time. Angle of attack of wing, 3.5°; indicated airspeed, 155 mph; natural normal-to-chord bending frequency of wing, 755 cpm; aileron frequency, 800 cpm; flutter frequency, 770 cpm.